



Contents lists available at <http://qu.edu.iq>

Al-Qadisiyah Journal for Engineering Sciences

Journal homepage: <https://qjes.qu.edu.iq>



Temperature change in steel-concrete composite bridge: Experimental and numerical study

Maryam Salim. A and Muhaned A. Shallal*

Department of civil engineering, College of Engineering, University of Al-Qadisiyah, Iraq.

ARTICLE INFO

Article history

Received 29 March 2021

Received in revised form 10 May 2021

Accepted 21 June 2021

Keywords

Composite Bridge

Solar radiation

Finite element analysis

Air Temperature

Temperature distribution

ABSTRACT

In this article, a prototype empirical section of the composite girder was performed to verify the temperature distributions and the changes in concrete bridges under environmental thermal stresses. T-Beam composite section was placed directly subjected to environmental conditions to endure the change in convection, the convection includes solar radiation, surrounding air temperature, and wind speed. In addition, this paper includes the 3D finite-element thermal studies represented by the COMSOL MULTIPHYSIC program, with particular reference to the influence of several parametric studies that are represented by changes in concrete thickness, adding asphalt layer, and finally change the value of wind speed. The section is prepared with fifteen thermocouples in different places in steel and concrete in the actual and theoretical models to evaluate the temperature distribution inside the composite bridges and their effects in the selected points. COMSOL MULTIPHYSIC showed a good ability to simulate convection, heat conduction, and radiation within the surrounding environment. Such as the thermocouple (TC3) the minimum temperature was 33.18 °C, 33.29 °C, the maximum temperature was 63.67 °C, and 62.77 °C for experimental and theoretical results respectively while the maximum and minimum difference between experimental and FE temperatures is 2.96 and 0.099 for TC3 respectively. Therefore, it can be said that all the thermocouples results showed a good agreement between practical and theoretical results.

© 2021 University of Al-Qadisiyah. All rights reserved.

1. Introduction

Continuous bridge girders undergo frequent heating and cooling cycles from the environment represented by sun radiation, and surrounding air temperature and these conditions produce thermal stresses. Thermal stress effects have often been related to damage to steel-concrete bridge girders. The nonlinear temperature distributions that stand up in bridges are not effortlessly anticipated and are often taken into consideration in a simplified manner, which can also cause structural behavior troubles[1, 2]. Exposed

structures, for example, bridges, are constantly heat loss and gain from sun radiation, convection, and returning radiation to and from the surrounding air, which causes the difference in average bridge temperature and non-linear temperature distributions alongside the depth and the width of the structure[3, 4]. Depending on the end situations of the girder, these temperature variations and gradients can also cause longitudinal enlargement and Shrinkage, and the thermal loads caused stresses in

* Corresponding author.

E-mail address: mohanad.shallal@qu.edu.iq (Muhaned A. Shallal)



directions perpendicular to the longitudinal axis. So that, the temperature variant can purpose critical cracking and deflections[4–7].To calculate temperature gradients in composite bridge girders, the quantity of solar radiation absorbed from the surface, the value of wind speed, and the air temperature have to be recognized. The quantity of absorbed solar radiation is a function of the surface sun energy absorption. Wind speed, bridge route, and geometry are key elements. Many studies on the impact of wind speed [2, 8], bridge route [2, 9, 10], and geometric formation[2, 9, 11] had been found in the present-day literature, even as exact parametric studies of the effect on temperature differences and distributions were found in concrete –steel girder. The purpose of this study is to show the result of the experimental study, and the results of the theoretical study by using the COMSOL MULTIPHYSIC program and a comparison between practical and theoretical results finally using several parametric to study the combined effect of changing concrete slab, adding asphalt layer and change the value of wind speed on the temperature gradients in concrete bridges.

2. Experimental work

Experimental works included casting a segment of composite concrete steel. Fig.1 shows the dimensions and locations of thermocouples in the composite bridge section. The steel beam depth is 500 mm, the width of the flange is 250 mm and the thickness of the web and flange is 8 mm. Experimental work includes welding I-steel beams in distinct dimensions and with 8 bolts that had been used as shear connectors. After that, the plywood had been used to make the framework of the concrete slab. The thermocouples sensor is used in this section to degree the temperature distribution and its effect on a composite bridge at certain points the entire number of thermocouples that have been used were (15), (7) in concrete and it symbolized by (TC), (7) in steel and it symbolizes by (TS) and one between them is symbolized by (TCS).

Finally, the concrete was poured as shown in Fig.2, and aspects of the concrete slab and steel were completely secluded through the use of foam to make the sample as an internal bridge and prevent switching heat from those faces as shown in Fig.3.

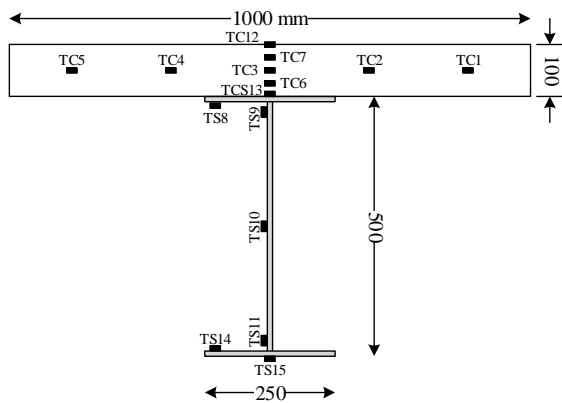


Figure 1. Dimensions and thermocouples locations.



Figure 2. Specimen after casting.



Figure 3. Secluded the sides of Specimen.

3. Experimental results

3.1. Environmental results

The environmental data were including measured three factors during July 24 that represent the summer season (sun radiation and daily air temperature are high in this season so; the temperature variance is high and clear). The first factor was surrounding air temperature, its essential in analyzing the thermal behavior of the model because it impacts the radiance of the exterior surface of the surroundings and the convective refrigeration over daylight hours. Fig.4 shows the behavior of the surrounding air temperature. The second factor was solar radiation and which indicates the external heat source. Fig.5 indicates the sun's radiation throughout 24 July. The most crucial factor affecting surface refrigeration by convection was wind speed, so the value must be known to take a look at the temperature gradients all through the day. Fig.6 shows the wind speed in the course of 24 July.

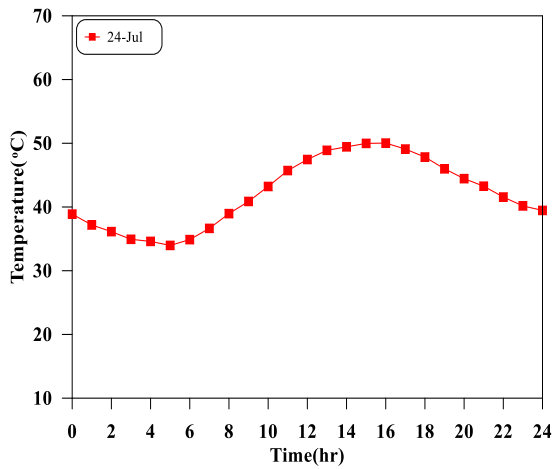


Figure 4. Ambient air temperature on 24 July.

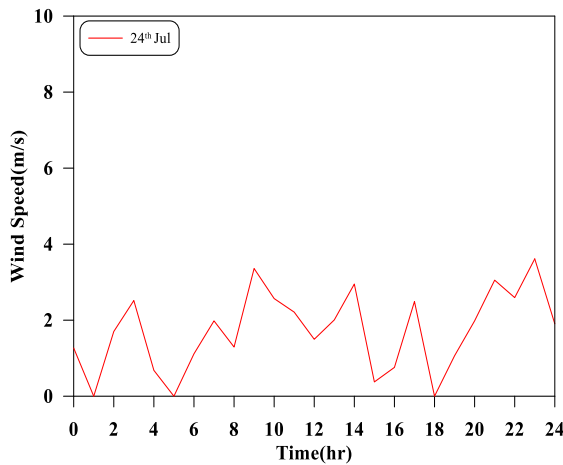


Figure 5. Solar radiation during 24 July.

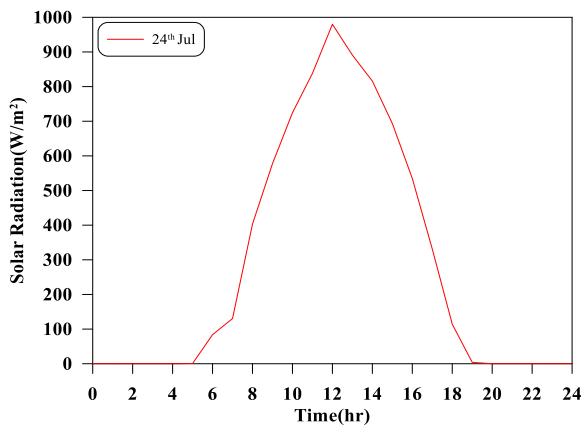


Figure 6. Wind Speed during 24-July

3.2. Temperature variance

Four thermocouples are used in this article to show the experimental results two thermocouples are used in concrete (TC3 and TC12) and two in steel (TS9 and TS11). In general, Fig.7 & Fig.8 show the temperature variance in concrete during the Sunny day (24 July). The figures show a clear variance during the Sunny day (24 July). Table 1 indicates the maximum and minimum recorded temperature distribution for TC3&TC12.

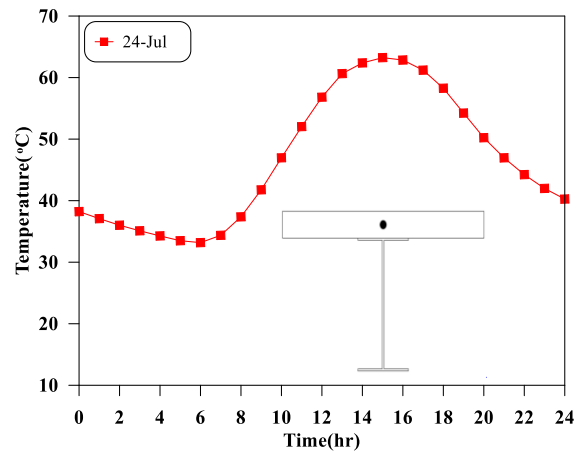


Figure 7. Temperature change in (TC3) thermocouple during a Sunny day.

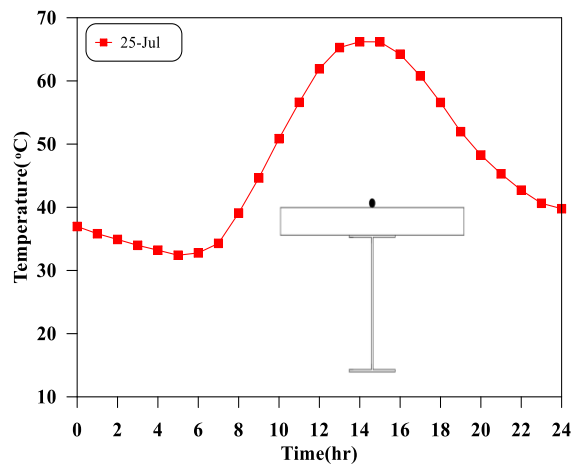


Figure 8. Temperature change in (TC12) thermocouple during a Sunny day.

Table 1. Minimum and maximum temperatures 24 July for TC3 and TC12.

Thermocouple	Minimum temperature (°C)	Maximum temperature (°C)
TC3	33.14	63.77
TC12	31.83	66.77

While Fig.9 & Fig.10 show that, the thermocouple in steel has jumps and these jumps came when the solar radiation becomes horizontal and falls directly on the steel section. Table 2 showed the maximum and minimum temperature distribution for TS9& TS11.

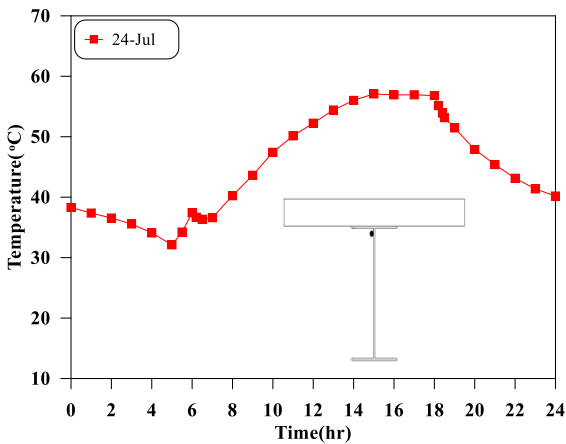


Figure 9. Temperature change in (TS9) thermocouple during a Sunny day.

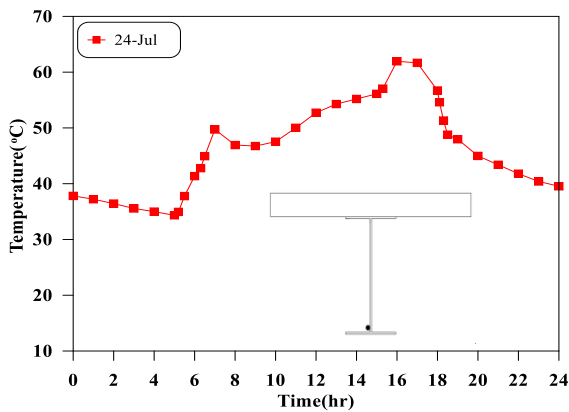


Figure 10. Temperature change in (TS11) thermocouple during a Sunny day.

Table 2. Minimum and maximum temperatures 24 July of thermocouple in steel.

Thermocouple	Minimum temperature (°C)	Maximum temperature (°C)
TS9	33.95	60.64
TS10	34.2	63.22

4. Finite element approach

COMSOL MULTIPHYSICS Mussa et al. [4] finite element software version 5.5 was used to study thermal transfer analysis of temperature on the girder of a steel-concrete-composite bridge (T-beam) for a sunny day

Fig.11 shows the mesh of composite bridge segment and Fig.12 shows the definition of solar location with respect to composite segment. It was assumed that the material properties that were used in the finite element analysis are isotropic and time-independent. In previous studies by Emanuel et al. [12], the material properties were set, so that the specified values could efficiently simulate the real heat transfer technique. The Concrete material properties are density $\rho = 2400$ (kg/m³), thermal conductivity $k = 1.5$ (W/m.K), and heat capacity at constant pressure (specific heat) $c = 900$ (J/kg.K). Steel material properties are density $\rho = 7850$ (kg/m³), thermal conductivity $k = 44.5$ (W/m.K), and heat capacity at constant pressure (specific heat) $c = 475$ (J/kg.K). Apply air temperature, wind speed, and vertical and horizontal solar radiation at a distinctive time to represent the initial temperature of the entire bridge body at the start of the FE analysis procedure.

The analysis was started 24 hours before the scheduled time to decrease the effect of the initial temperature on the solution and to avoid errors in the COMSOL program.

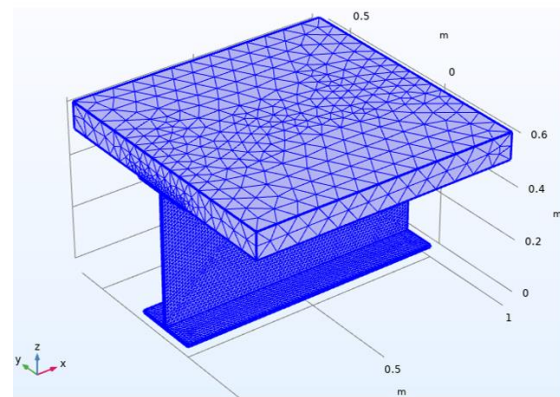


Figure 11. The mesh of the composite bridge segment.

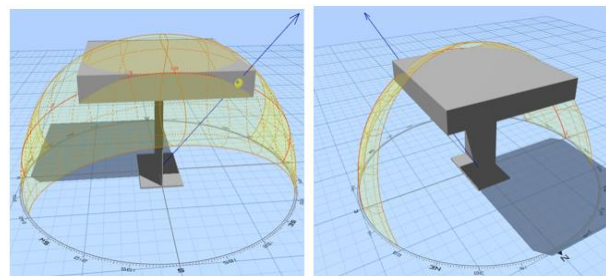


Figure 12. The definition of solar location with respect to composite segment.

4.1. Comparison Between Practical and Numerical Results

The chosen day, July 24, 2020, is used to conduct a comparative study of the temperatures recorded from the experimental composite steel bridge girder section and the temperatures predicted from FE thermal analysis. Four thermocouples are used to show the experimental and theoretical results, two thermocouples are used in concrete (TC3 and TC12) and two in steel (TS9 and TS11). In general, Fig.13 to Fig.16 shows the result of the

TC3, TC12, TS9, and TS11 thermocouples that showed a good match between the experimental temperature result and the finite element temperature result. For this reason, it can be concluded that the FE model is effective. The TC3 and TC12 thermocouples located in the middle concrete slab and the top of the concrete slab respectively, Fig.13 and Fig.14 illustrate the comparison between the experimental results and the finite element results. From this figure, the general behavior of the time-varying temperatures was nearly identical between the experimental results and the FE results. Table 3 shows a comparison of the minimum and maximum temperatures for sunny days (July 24) for these thermocouples. The maximum difference between experimental and FE temperatures is 2.96 and 2.34 for TC3 and TC12.

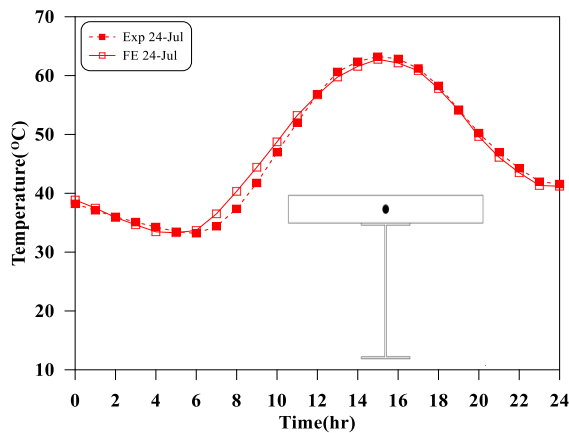


Figure 13. Hourly experimental recorded and FE expected temperatures at TC3 thermocouple of a composite segment.

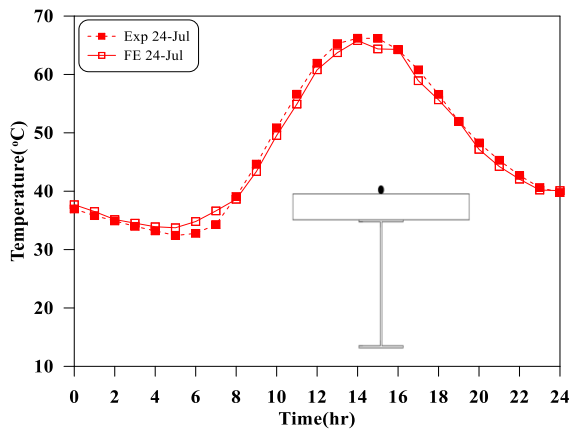


Figure 14. Hourly experimental recorded and FE expected temperatures at TC12 thermocouple of a composite segment.

Table 3. Minimum and maximum temperatures 24 July for TC3 and TC12.

Thermocouple	Min. temperature (°C)		Max. temperature (°C)	
	Experimental	FE	Experimental	FE
TC3	33.18	33.29	63.67	62.77
TC12	32.41	33.74	66.2	65.80

The thermocouples TS9 and TS11 are located in the steel web also in different places, Fig.15 & Fig.16 indicates the comparison between the experimental results and the results of FE. The general behavior of the figures showed a good match between practical and theoretical results. Table 4 shows a comparison of the minimum and maximum temperatures for sunny days (July 24) for these thermocouples. The maximum difference between experimental and FE temperatures is 1.78 and 2.54 for TS9 and TS11.

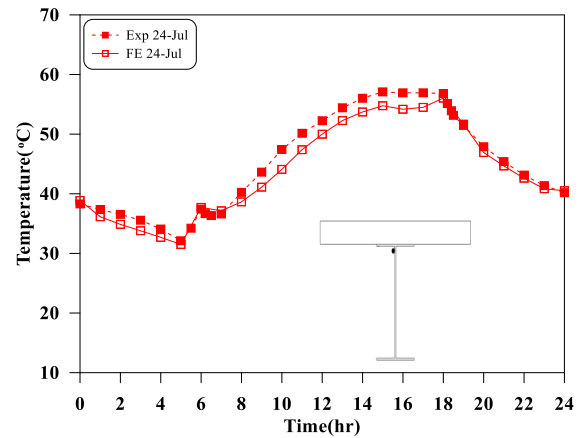


Figure 15. Hourly experimental recorded and FE expected temperatures at the TS9 thermocouple of the composite segment.

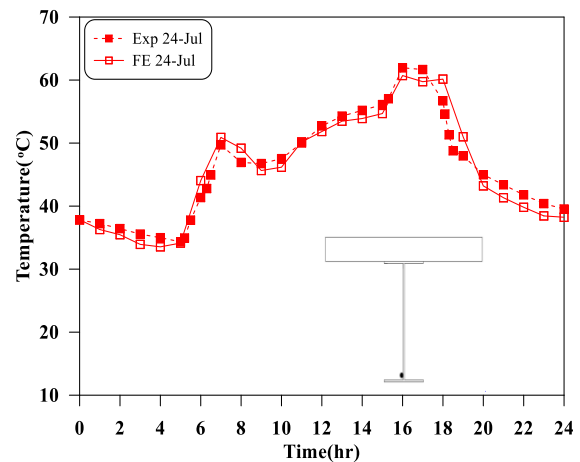


Figure 16. Hourly experimental recorded and FE expected temperatures at the TS11 thermocouple of the composite segment.

Table 4. Minimum and maximum temperatures 24 July of thermocouple in steel.

Thermocouple	Min. temperature (°C)		Max. temperature (°C)	
	Experimental	FE	Experimental	FE
TS9	32.12	31.51	57.09	56.05
TS11	34.34	33.54	61.95	60.72

5. Parametric study

Several parametric studies were performed to verify the effects of concrete slab thickness, change the value wind and use an asphalt layer on the temperature distribution of the composite section. Presumably, the studied bridges are located in Diwaniyah, Iraq (32 00N, 4455E). Two days were chosen to study the various parametric studies, and these days represent the extremes of weather conditions (24 July 2020 and 15 January 2020), and the same weather data obtained from the experimental work for these days were adopted. For all parametric studies, the average wind speed value was used which is equal to 1.232 (m/s) for the winter and it is equal to 1.712 (m/s) for the summer. The real part of one of the spans inside the Abu Al Fadl Bridge, as shown in Fig. 17, was approved in the city of Diwaniyah, to study the effect of parametric studies on temperature change.

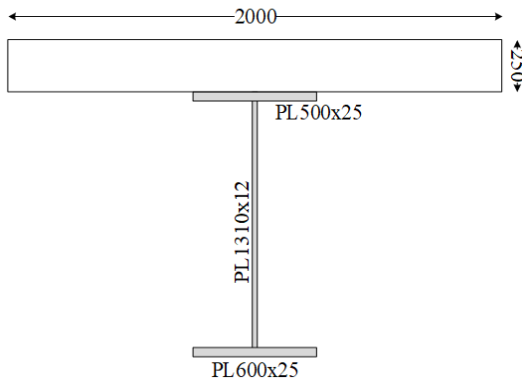


Figure 17. Dimensions of the bridge section.

5.1. Effect of slab thickness

Concrete slab thickness in composite bridges is an important factor affecting the temperature gradient within the segment. To study the effect of this parameter, four values were chosen to represent the thickness of the concrete slab 150, 200, 250, and 300 mm, with no change in steel dimension.

Fig.18 shows the temperature change during the day at the upper surfaces of the concrete on a hot day (July 24) and a cold day (January 15) respectively. From Fig.18 it can be seen that the temperature of the upper surface is not affected by the change in the thickness of the concrete slab on summer and winter days, because changes in concrete thickness do not affect the amount of energy exchanged between the upper surface and the surrounding atmosphere. Fig.19 shows an increase in the effect on the temperature of the bottom surface when the thickness of the concrete slab decreases on a hot day, while this effect decreases on a cold day, and the reason is due to the closing of the distance between the two. So the lowest concrete surface is affected more than another surface. The difference in surface temperature and temperature in the concrete core is an important factor in determining the temperature distribution. Fig.20 indicates the effect of the change in thickness on the difference between upper surface temperature and temperature at 60 % and 80% from the depth of concrete slab thickness on a hot and cold day (24 July, 15 January). From Fig.20, the maximum temperature differences are on 24-July 15.44 °C, 18.29 °C, 20.48 °C, and 22.34 °C, and occur between 12:00 and 12:45, the temperature extremes from January 15 are 4.27 °C, 4.49 °C, 4.77 °C, and 5.10 °C, and occurred between 14:00 and 14:30 for the thickness of 150, 200, 250, and 300 mm straight. The minimum temperature differences on July 24 were

2.37 °C, 3.23 °C, 4.04 °C and 4.70 °C and occur between 0:00 and 4:30 for thicknesses of 150, 200, 250, and 300 mm, respectively for 60% from concrete depth. While for 80% of concrete, in Fig. 21 the temperature extremes are from July 24 to 18.09 °C, 20.60 °C, 22.34 °C, and 24.09 °C, and occur between 12:00 and 12:45 for the thickness of 150, 200, and 250, and 300 mm, respectively. The temperature extremes were from January 15 to 4.82 °C, 5.21 °C, 5.50 °C and 5.85 °C, and occurred between 14:00 and 14:30 for thicknesses of 150, 200, 250, and 300 mm straight. The minimum temperature differences on July 24 were 1.49 °C, 1.99 °C, 2.41 °C and 2.91 °C, and occurred between 0:00 and 4:30 for thicknesses of 150, 200, 250 and 300 mm, respectively. The differences in minimum temperatures on January 15 were 1.26 °C, 1.89 °C, 1.95 °C, and 2.66 °C, and occur at 5:15 pm for thicknesses of 150, 200, 250, and 300 mm, respectively. From the above data for the two figures, a set of observations can be recorded, where the temperature difference rises with the rises in the thickness of the slab, and the maximum difference occurs on a hot day (July 24) at noon, as well as the minimum difference that occurs on the same day.

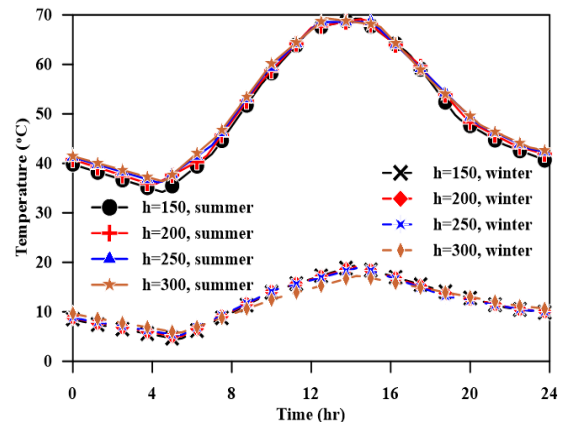


Figure 18. Effect of slab thickness on the top surface temperature in 24-July and 15-January.

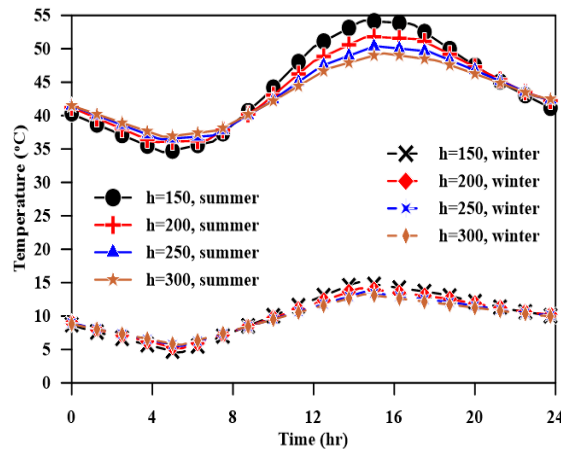


Figure 19. Effect of slab thickness on the bottom surface temperature in 24-July and 15-January.

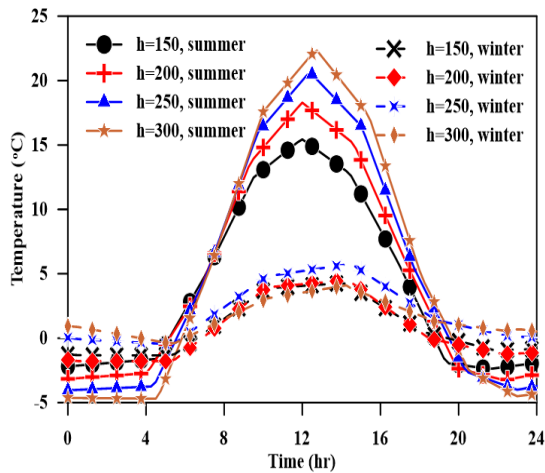


Figure 20. Effect of thickness on the variance between the upper surface temperature and the temperature at a depth of 60% of the slab thickness.

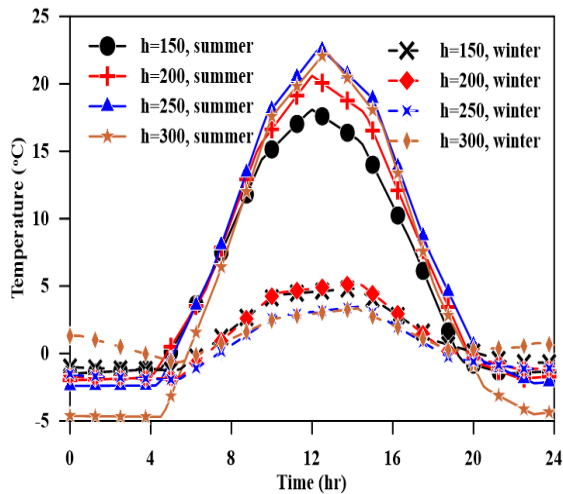


Figure 21. Effect of thickness on the variance between the top surface temperature and the temperature at a depth of 80% of the slab thickness.

Fig.21 shows the temperature gradients are linear and positive between the top surface and 80% of the concrete slab thickness, at the same time as its miles negative between the bottom surface and 80% of the concrete slab thickness. Fig.22 indicates that the reversed temperature distribution is concave, and the temperatures of the upper and lower surfaces are approximately identical. Table 5 shows the effect of slab thickness at the maximum and minimum average temperatures of the composite bridge. The maximum temperature became recorded on July 24 between 14:30 and 15:30, whilst the minimum average temperature turned into recorded on January 15 at 15:15. The distinction between the maximum and the implied minimal temperature is 54.84 ° C, 51.80 ° C, 49.48 ° C, and 47.61 ° C for the thickness of the slab is 150, 200, 250, 300 mm respectively.

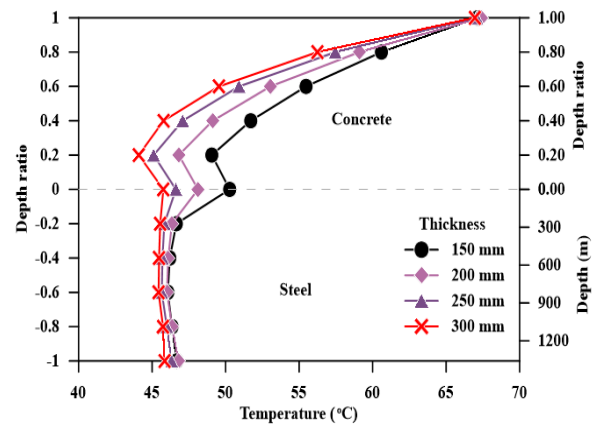


Figure 22. Thickness effect on temperature gradient at noon hr on (24-July).

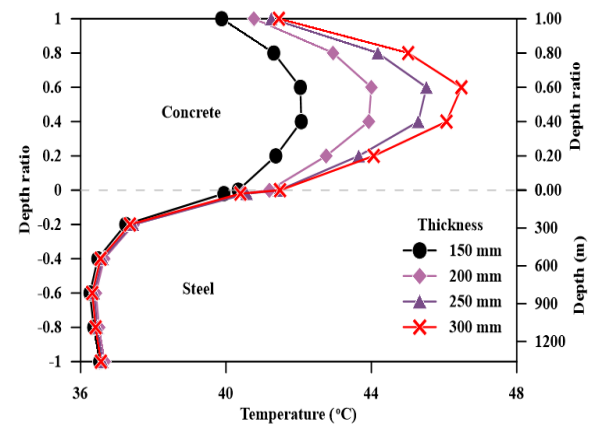


Figure 23. Thickness effect on temperature gradient at 0:00 hr on (24-July).

Table 5. Effect of slab thickness on the maximum and minimum average temperature of the composite bridge.

Thickness (mm)	Maximum (°C)	Time (hr)	Minimum (°C)	Time (hr)	Range (°C)
150	59.69	14:30	4.85	5:15	54.84
200	57.57	14:45	5.77	5:15	51.80
250	55.97	15:00	6.49	5:15	49.48
300	54.63	15:30	7.02	5:15	47.61

5.2. Effect of asphalt thickness

Several parametric studies are performed to discuss the effects of varying convection. One of these parameters was the effect of the asphalt layer. The different values of thickness of the asphalt were used and these values were 0, 6, and 10 cm. A zero value of asphalt layer thickness means no asphalt layer, the concrete slab is the surface exposed to solar radiation. The

properties of asphalt material are solar absorption coefficient $a = 0.92$, density $\rho = 2100 \text{ (kg / m}^3\text{)}$, thermal conductivity $k = 1.1 \text{ (W /m.K)}$, specific heat $c = 920 \text{ (J / kg. K)}$, and emissivity coefficient ($\epsilon = 0.93$).

Fig.24 shows the temperature difference of the top surface of the concrete. In summer, it can be seen that the temperatures of the top surface of the sample, which is 6 cm thick, are approximately the same as that of the sample not covered by asphalt, with a time difference between the two curves. The temperatures of a sample covered with asphalt with a thickness of 10 cm are lower than other samples. The reason is due to the greater depth of asphalt compared to another sample which means that the amount of heat that reaches the surface of the concrete is less compared to the sample that has a thickness of 6 cm. During the night, samples covered with asphalt retain heat compared to samples without asphalt, as the upper surface is not subjected to direct cooling at night. In winter, the effect is almost negligible, and the reason is the small amount of solar radiation during this period of the year.

Fig.25 and Fig.26 show the temperature gradients with the depth of the bridge installed at 15:00 and 1:00, respectively. Fig.25 indicates the temperature difference inside the concrete slab ranges from approximately 0.5 to 3 °C when comparing the sample covered with a 6 cm asphalt layer with the reference sample (without the asphalt layer), while the difference is greater when comparing the reference sample with the sample covered with an asphalt layer 10 cm long. Fig.25 shows that the temperature difference is concentrated inside the top of the concrete slab. This difference is limited when the sample covered with a 6 cm asphalt layer is compared with the reference sample (without the asphalt layer), while the difference is clear and tangible when comparing the reference sample with the sample covered with a layer of Asphalt 10 cm long. Fig.26 indicates the effect of adding an asphalt layer on the maximum and minimum average temperature of the composite bridge. Table 6 shows the average maximum and minimum temperatures for the composite bridge for the different asphalt layers. The differences between the maximum and minimum average temperatures decrease slightly with the increase in the thickness of the asphalt layer.

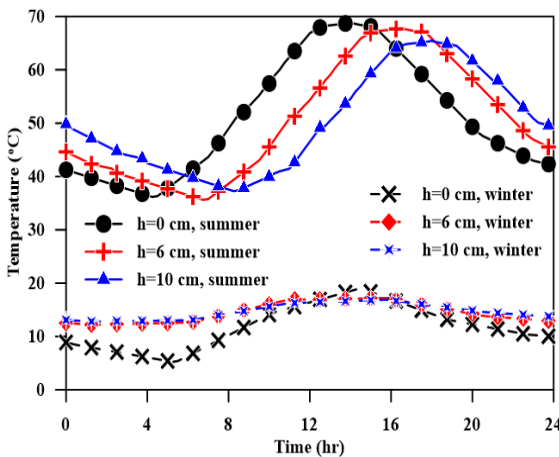


Figure 24. Effect of asphalt layer thickness on the temperature of the concrete top surface.

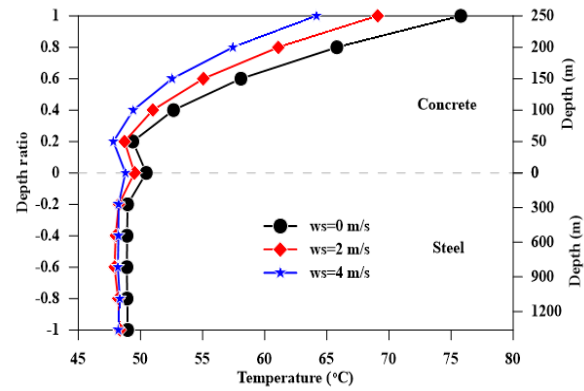


Figure 25. Effect of asphalt layer thickness on the temperature distribution with a depth of the composite bridge at hr=15:00.

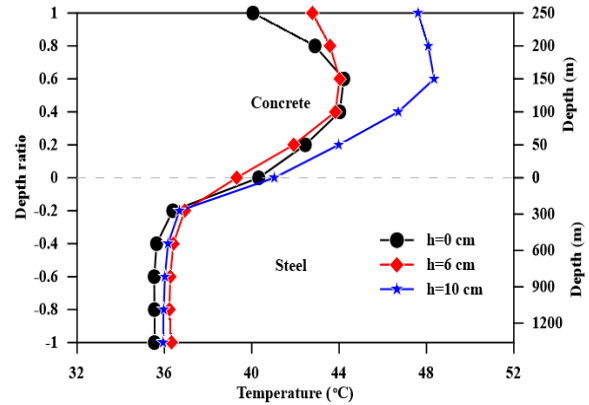


Figure 26. Effect of asphalt layer thickness on temperature distribution with the depth of the composite bridge at hr=1:00.

These results are in accordance with the British standard BS 5400-2 [13], where the presence of an asphalt layer with a thickness of 100 mm reduced the differences between the maximum and minimum average temperatures to 3 °C, while the results of the current study showed the difference between the maximum The minimum average temperature is 4.18 °C for the same thickness (100 mm). AASHTO [14] considered that these differences due to the asphalt layer are small and can be neglected. Fig. 27 shows the effect of the asphalt layer on the maximum and minimum average temperature of the composite bridge.

Table 6. Effect of an asphalt layer on the maximum and minimum average temperature of the composite bridge.

Asphalt thickness (mm)	Maximum (°C)	Time (hr)	Minimum (°C)	Time (hr)	Range (°C)
0	55.97	12:45	6.49	5:15	49.48
60	54.92	15:15	6.83	5:30	48.1
100	53.02	15:45	7.72	5:30	45.3

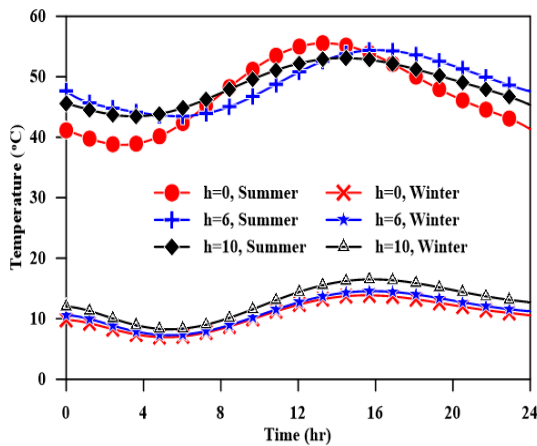


Figure 27. Effect of an asphalt layer on the maximum and minimum average temperature of the composite bridge.

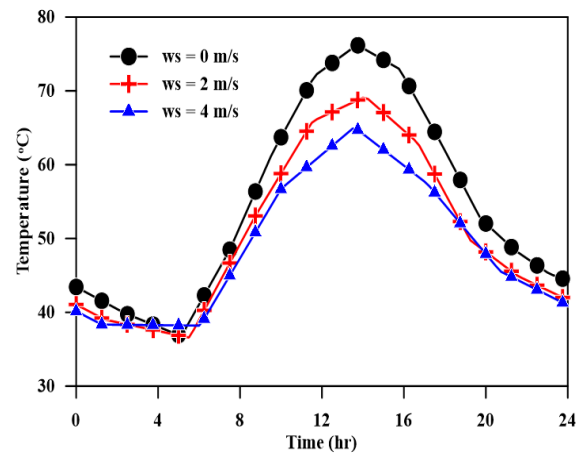


Figure 28. Effect of wind speed on the temperature variation of the top surface concrete slab on a summer day (24 July).

5.3. Effect of wind speed

The third parameter was to study the effect of wind speed on the temperature gradient. Wind speed affected the heat transfer coefficient (h_c). Three different values of wind speed were used and these values are 0, 2, and 4 (m/s). Fig.28 and Fig.29 show the effect of wind speed on the temperature change of the top and bottom surface of the concrete slab on (July 24). From the figure, it can be seen that the temperature decreases with increasing wind speed where the maximum difference in temperature is 7.78 and 12.60 °C for the upper surface and the difference for the lower surface was 2.76 °C and 3.67 ° when comparing the temperature curves of wind speed 2 and 4 (m/s) with the wind speed curve temperatures equal to zero, respectively. The maximum differences between the temperature curves appeared at 15.45 for the top and appeared at sunset for the bottom surface. Fig.30 shows the impact of wind speed on the temperature gradient of the composite bridge at 14:00 (July 24). From this figure, it could be observed that the maximum difference between the temperature curves occurs at the top surface of the concrete slab, and the temperature gradient will increase with the decrease in wind speed. Fig.31 shows the effect of wind speed on the average maximum and minimum temperature of the composite bridge, while Table 7 shows the average maximum and minimum temperature of wind speeds 0, 2, and 4 m / s. From the above figure and table, it could be observed that the wind speed has no effect in the winter season, but in the hot season, the wind speed is influential in the maximum mean temperature as the average temperature decreases with increasing wind speed.

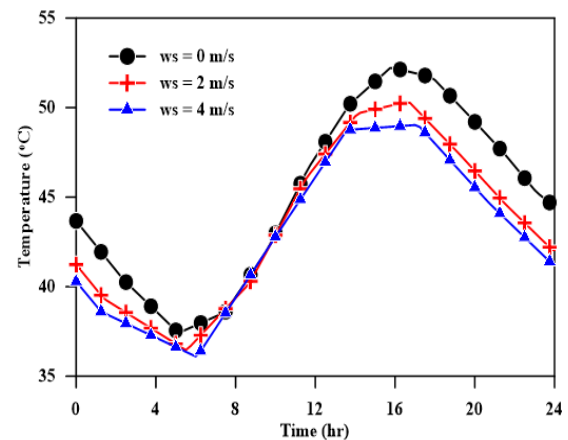


Figure 29. Effect of wind speed on the temperature variation of the bottom surface concrete slab on a summer day (24 July).

Table 7. Effect of wind speed on the maximum and minimum average temperature of the composite bridge.

Wind Speed (m/s)	Maximum (°C)	Minimum (°C)	Range (°C)
0	59.86	6.55	53.13
2	55.94	6.44	49.05
4	52.64	6.43	46.21

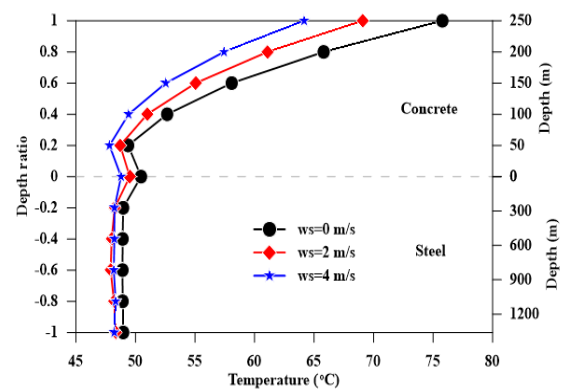


Figure 30. Effect of wind speed on the temperature gradient in the composite section on a summer day (24-July @ 14:00).

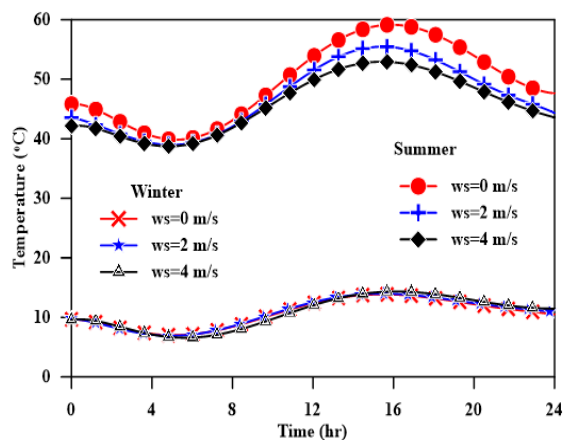


Figure 31. Effect of wind speed on the maximum and minimum average temperature.

6. Conclusion

Based on the data estimated from the composite section analysis under the environmental conditions of Iraq weather using the COMSOL MULTIPHYSICS program and from the practical results, the following conclusions can be drawn:

6.1. Experimental Conclusions

1. The maximum air was 50.03 °C while the daily minimum value was 4.09 °C so, the difference between the two values was, 45.94 °C. The maximum solar energy of 24 July was 980 (W/m²), while the minimum sun radiation appeared on cold days and its value was 498.7 (W/m²)
2. The temperature variance is clear during the hot day (24 July)
3. The thermocouple within the steel segment has jumped within the measured temperature, and this temperature increase is throughout the duration of sunrise and sunset due to the exposure of the steel section to direct sunlight.

6.2. The Numerical Conclusions

1. The FE model using COMSOL MULTIPHYSICS of the composite section showed a good ability to simulate convection, thermal conductivity, and radiation within the surrounding environment. Therefore, the thermocouples showed good agreement between FE and the experimental results.
2. The numerical study showed that the thickness of the concrete slab has no effect on the temperature of the top surface, while the effect of the thickness of the concrete slab is noticeable on the temperatures of the bottom surface of the concrete slab and the temperatures inside the concrete slab.
3. Existing asphalt layer leads to an increase in the solar energy gained during the day due to the black color of the layer, but on the other hand, the presence of the asphalt layer with a certain thickness will lead to lower temperatures at the bottom surface of the asphalt layer, so the presence of a medium thickness layer (50 or 60 mm) has a

slight effect on the temperatures of the top surface of the concrete slab during the day while the increase in thickness of this layer leads to a decrease in the temperature of the top surface of the concrete.

4. During the day, when comparing the top surface temperature of a composite segment without an asphalt layer with the compound section of the asphalt layer thickness of 60 mm, the temperature difference is less than 2 °C, while when the layer thickness is 100 mm, the difference is more than 9 °C. While at night, noticed the opposite, as the temperatures are hotter when there is an asphalt layer and the temperature increase during this period with the increase in the thickness of the layer as a result of not cooling the concrete surface by the wind when covering the concrete surface with an asphalt layer
5. Increasing wind speed cools the surface, and vice versa. The maximum temperature difference of the upper concrete surface is 7.78 and 12.60 °C when comparing the temperature curves of the wind velocity of 2 and 4 (m/s) with the wind velocity curve temperatures equal to zero, respectively. The influence of wind speed is less on other areas of the compound section.
6. From the parametric study the maximum effect can be obtained during the hot day when the solar energy absorbed by the concrete surface is higher while the steel part is shaded by the overhanging parts, the wind speed is lower, and the air temperature range is high. Based on these conditions, an effective temperature of 60 °C may be recommended for bridges whose concrete slab thickness is 200 mm or less. While for bridges with concrete slabs greater than 200mm, 55 °C is recommended as the effective temperature.

Authors' contribution

All authors contributed equally to the preparation of this article.

Declaration of competing interest

The authors declare no conflicts of interest.

Funding source

This study didn't receive any specific funds

REFERENCES

- [1] R. A. Imbsen, D. E. Vandershaf, R. A. Schamber, and R. V. Nutt, *Thermal Effects in Concrete Bridge Superstructures.*, (3). Washington, DC., 1985.
- [2] M. M. Elbadry and A. Ghali, Temperature Variations in Concrete Bridges, *Journal of Structural Engineering*, 109(10) (1983) 2355–2374.
- [3] G.-D. Zhou and T.-H. Yi, Thermal Load in Large-Scale Bridges: A State-of-the-Art Review, *International Journal of Distributed Sensor Networks*, 9(12) (2013) 217983.
- [4] F. Mussa, S. R. Abid, and N. Tayşi, Winter temperature measurements in a composite girder segment, *IOP Conference Series: Materials Science and Engineering*, 888 (2020) 012074.
- [5] P. D. Krauss and E. A. Rogalla, *TRANSVERSE CRACKING IN NEWLY CONSTRUCTED BRIDGE DECKS*, (1996) 132.
- [6] M. Elbadry and A. Ghali, Control of thermal cracking of concrete structures, *ACI Materials Journal*, 92(4) (1995) 435–450.
- [7] M. Elbadry and A. Ghali, Thermal Stresses and Cracking of Concrete Bridges, *ACI Journal Proceedings*, 83(6) (1986) 1001–1009.
- [8] B. Wang, W. Wang, and X. Zeng, Measurement and analysis of temperature effects on box girders of continuous rigid frame bridges, *World Academy of Science, Engineering and Technology*, 46(10) (2010) 731–737.
- [9] W. H. Dilger, A. Ghali, M. Chan, M. S. Cheung, and M. A. Maes, Temperature Stresses in Composite Box Girder Bridges, *Journal of Structural Engineering*, 109(6) (1983) 1460–1478.

-
- [10] C. W. Roeder, Thermal Movement Design Procedure for Steel and Concrete Bridges .Report to the National Cooperative Highway Research Program, (April). Washington, D.C., 2002.
- [11] D. Li, M. A. Maes, and W. H. Dilger, Thermal design criteria for deep prestressed concrete girders based on data from confederation bridge, *Canadian Journal of Civil Engineering*, 31(5) (2004) 813–825.
- [12] J. H. Emanuel and C. M. Taylor, Length-thermal stress relations for composite bridges, *Journal of Structural Engineering (United States)*, 111(4) (1985) 788–804.
- [13] British Standards Institution BSI, Steel, concrete and composite bridges - Part 2. Specification for loads, BS 5400-2: (2006) 32–34.
- [14] AASHTO, AASHTO LRFD Bridge Design Specifications, 8th Edition - Table of Contents and Introduction, (2017).